Tectonophysics, 152 (1988) 227–237
Elsevier Science Publishers B.V., Amsterdam – Printed in The Netherlands

Two dilatancy-based models to explain coda-wave precursors and P/S spectral ratio

A.A. GUSEV

Institute of Volcanology, Petropavlovsk–Kamchatsky, 683006 (U.S.S.R.)

(Received December 15, 1986; accepted November 17, 1987)

Abstract

Gusev, A.A., 1988. Two dilatancy-based models to explain coda-wave precursors and P/S spectral ratio. In: O. Kulhánek (Editor), Seismic Source Physics and Earthquake Prediction Research. *Tectonophysics*, 152: 227–237.

Some coda-wave precursors can be predicted by the dilatancy model. Others need more complicated models. The first of the models proposed here takes into account the compression of the medium around the swelling dilatancy zone, and explains several observed precursor properties. A simple theoretical model is employed to describe anisotropic S-wave absorption in a microcracked medium under shear load. The second model is used to explain the radiation bursts observed in coda in the preparation period, and which overlap background scattered waves. This model also explains the unusually high P/S energy ratio of seismic waves from shocks in preparation zones. The concept of seismic emission is employed to explain these phenomena. Two possible modes of emission are proposed: (1) "passive" radiation generated by an abrupt dilatancy drop produced by stress drop in and around the earthquake source, and (2) "active" radiation stimulated by seismic waves in a preparation zone, or in any other volume of the lithosphere which is in a state of changing dilatancy.

Introduction

In several recent studies, temporal variations have been found in the coda wave parameters of small earthquakes that occurred in regions where large earthquakes were in preparation (Malamud, 1974; Gusev and Lemzikov, 1980; Jin and Aki, 1986). Some of these variations are in general agreement with the predictions of the usual dilatancy theory, and are probably produced by an increase in S-wave absorption due to microcracking. The regular patterns found for these and other precursors seem to indicate that the compression of the Earth's medium due to the swelling dilatancy zone must also be taken into account.

This approach has proved useful, but leaves some coda wave phenomena unexplained. Considered as isolated facts, these phenomena are difficult to explain. They can be compared, however, with the well-known P/S spectral ratio anomaly of earthquakes, remembering that this anomaly is especially pronounced for shocks from preparation regions. These data as a whole can be tentatively explained in terms of the idea of an active medium. We suppose that the medium in a preparation zone is overburdened with strain energy and is capable of radiating elastic waves spontaneously or under excitation. The proposed mechanism of this excitation is the rapid dilatancy change. The combination of the two models appears to explain many details of coda anomalies, and some other precursory effects as well.

The concentric model of preparation region

To explain the nature of earthquake precursors, various hypotheses based on the general concept of dilatancy of the Earth's medium have been suggested (Scholz et al., 1973; Crampin et al.,

0040-1951/88/$03.50

1984). Dilatancy can be approached on two levels, namely the macroscopic level, dealing with non-Hookean volume change (increase) under shear stress, and the microscopic level, dealing with the formation of microcracks in rock specimens. These are mainly tensile cracks, and their orientation is related to that of a stress tensor. Dilatancy is most prominent under loads which are near to the critical fracturing stress. If one assumes that the tectonic load which causes the fracture in an earthquake source is of the order of kbar (Artyushkov, 1982) and that typical stress drops in earthquakes are below 100 bar, then the lithosphere in and around seismic zones is always under a near-critical load, so that dilatancy very probably occurs there continually (Nikolaevsky, 1982).

Therefore, it should be clear that we are here concerned with a special case of precursory dilatancy in regions of earthquake preparation, expressed in the growth of initial microcracks and/or the formation of additional microcracks (Crampin et al., 1984). This dilatancy leads to swelling of the dilatant volume, but is not the only cause of swelling in the preparation zone. Precursory creep can occur in some parts of a fault zone and can lead to an additional increase in volume as a result of the sliding of non-flat surfaces. One way or another, an increase in volume around the source of a future earthquake seems to be fairly likely.

No consensus exists at present about the extent of dilatancy zones. On the basis of observational data, we shall assume that the dimension of this zone is not less than the dimension of the source of an impending earthquake, and can be several times greater.

In dilatancy experiments with rock specimens, conditions of constant background hydrostatic pressure are typical. In the Earth the boundary conditions are different, in that the dilatancy zone is surrounded by an effectively elastic medium that resists free swelling. Near the surface, however, swelling in an upward direction can occur much more freely. So swelling in the Earth will be weaker than in the case of a laboratory model under constant pressure, while the medium surrounding the dilatancy zone will be considerably compressed.

For an effectively elastic environment, the picture arising from these considerations can be described roughly as a cavity whose boundaries are loaded with hydrostatic pressure. Qualitatively, the picture can be reduced to the formation of two concentric zones, an inner "dilatancy zone" and an outer "compression zone" with no clear external boundary. The additional stress and strain in the compression zone will decrease with increasing distance from its boundary with the dilatancy zone roughly with r^{-3}, where r is the distance from the centre of the source of the impending earthquake.

When a dilatancy zone is situated near to the free surface of the Earth, this relatively simple concentric picture will be distorted. We shall take this into account below. Another complication is related to the varying capability of the Earth's materials to dilate at different depths and lateral locations. Following Nikolaevsky (1982), as an initial approximation, isotherm 600 °C will be considered as the lower boundary of potential dilatancy. For island arc earthquakes the shape of this isotherm on the cross section of the arc is rather complicated, and the zone of possible dilatancy should reflect this complicated shape.

It is clear that dilatancy microcracks exist not only in the dilatancy zone, but also in the compression zone, where precursory dilatancy is absent. We shall assume that this microcracking leads to only minor deviations from Hooke's law in the material of the outer zone. Microcracks in this zone will, however, react to compression, therefore the "active" additional microcracking in the dilatancy zone will produce a "passive" decrease in the effective microcrack density in the compression zone. Therefore we would expect all precursors related to microcracking in these two zones to have the same time dependency, but an opposite sign of anomaly.

As macroscopic effects will increase when cracks grow in number and in size and will decrease in the opposite case, we can formally introduce the concept of a standard microcrack and consider an equivalent density of these microcracks as the effective microcrack density. This density will increase in the dilatancy zone, and will decrease in the compression zone.

It should be noted that our conclusion about the opposite phase character of anomalies in the inner and outer zone is valid only for effects which depend on the average microcrack density. Other effects which depend on crack anisotropy (e.g. preferred orientation of normals to crack planes) also need to be taken into account. Behaviour of this kind cannot be predicted from general considerations (corresponding calculations are given in the next section).

Signs of some anisotropic dilatancy effects

In this section, a simple quantitative approach will be proposed to model the effects of anisotropic dilatancy on shear wave propagation. We shall confine ourselves to the case of a homogeneous stress field. The main aim of the calculation will be to find a qualitative estimate of the average anisotropic absorption of elastic shear waves in a microcracked medium under load.

Let us briefly consider the relevant physical processes. We suppose that cracks are small compared to the wavelength of the propagating shear wave. Hence, the alternating stress field of the wave can be assumed to be homogeneous near the crack. Under this stress, cracks change in shape and volume, and wave energy is lost during this deformation (because of wet surface effects, non-adiabatic fluid compression–expansion cycle etc.). Thus, some wave absorption takes place. At the same time, elastic moduli decrease, and wave velocities decrease too. These effects depend on the degree of wave-crack interaction. We will assume that all these effects are determined by the value of normal stress amplitude of the elastic wave, which is produced in a medium with a "glued" crack in the area corresponding to the crack surface. Formally, we postulate the following:

(1) The amplitude of the (vector) normal stress on the (closed) crack surface with unit normal $\boldsymbol{n}$ is:

$$\tilde{\sigma}^{(n)} = \tilde{\sigma}_{ik} n_i n_k \tag{1}$$

where the wave stress amplitude $\tilde{\sigma}_{ik}$ is:

$$\tilde{\sigma}_{ik} = \mu\left(k_i u_k^0 + k_k u_i^0\right) \tag{2}$$

where μ is the shear modulus, $\boldsymbol{k}$ is the wave vector, and $\boldsymbol{u}^0$ is the displacement amplitude. It is convenient to introduce unit vectors $\boldsymbol{\varkappa} = \boldsymbol{k}/|\boldsymbol{k}|$, $\boldsymbol{\eta} = \boldsymbol{u}^0/|\boldsymbol{u}^0|$ and the normalized wave stress:

$$s_{ik} = \varkappa_i \eta_k + \varkappa_k \eta_i \tag{3}$$

Its value on the (closed) crack surface is:

$$s^{(n)} = |s_i^{(n)}| = s_{ik} n_i n_k$$

(2) The effective crack density with normal $\boldsymbol{n}$ in solid angle $\mathrm{d}\Omega_n$ (per unit of volume) is $\rho(\boldsymbol{n})$.

(3) The dimensionless absorption Q^{-1} is proportional to $\rho(\boldsymbol{n})$ and to $[s^{(n)}(\boldsymbol{\eta}, \boldsymbol{\varkappa}, \mathbf{n})]^2$. Thus, summing with respect to $\mathrm{d}\Omega_n$, we can write:

$$Q^{-1}(\boldsymbol{\varkappa}, \boldsymbol{\eta}) = A \int_{\Omega_n} \left[s^{(n)}(\boldsymbol{\eta}, \boldsymbol{\varkappa}, \boldsymbol{n})\right]^2 \rho(\boldsymbol{n})\, \mathrm{d}\Omega_n \tag{4}$$

(4) The additional static stress σ_{ij} leads to a change in the crack density $\rho(\boldsymbol{n})$. This change, $\Delta\rho$, is proportional to the normal load from σ_{ij} in an area with normal $\boldsymbol{n}$:

$$\Delta\rho(\boldsymbol{n};\ \sigma_{ij}) = B\rho_0(\boldsymbol{n})\sigma_{ij} n_i n_j \tag{5}$$

where $\rho_0(\boldsymbol{n})$ is the initial density.

(5) When wave scattering is considered, conversion scattering SV $\rightleftarrows$ SH (and, even more so, S $\rightleftarrows$ P) is neglected. Then, in order to estimate the average absorption $\overline{Q^{-1}}$ for scattered waves of a given polarization, we must find an average of such changes for different random ray directions $\boldsymbol{\varkappa}$. For SH waves, for example,

$$\overline{Q_{\mathrm{SH}}^{-1}} = \frac{1}{4\pi} \int_{\Omega_\varkappa} Q^{-1}(\boldsymbol{\varkappa}, \boldsymbol{\eta}_{\mathrm{SH}})\, p(\boldsymbol{\varkappa})\, \mathrm{d}\Omega_{\boldsymbol{\varkappa}} \tag{6}$$

where $p(\boldsymbol{\varkappa})$ is the probability density of the direction of a small standard segment of the ray on a unit sphere $\Omega_{\boldsymbol{\varkappa}}$.

Now, we can easily obtain the main formula representing the change ΔQ^{-1} of absorption Q^{-1} after applying the additional load to the medium. Substituting (5) into (4) we obtain:

$$\Delta Q^{-1}(\boldsymbol{\varkappa}, \boldsymbol{\eta}) = AB \int_{\Omega_n} \sigma_{ij} s_{kl} s_{mn} n_i n_j n_k n_l n_m n_n \rho_0(\boldsymbol{n})\, \mathrm{d}\Omega_n \tag{7}$$

where $s_{kl} = s_{kl}(\boldsymbol{\varkappa}, \boldsymbol{\eta})$. The difference in absorption for direct SV and SH waves depends only on $\boldsymbol{\varkappa}$:

$$D(\boldsymbol{\varkappa}) = \Delta Q_{\mathrm{SV}}^{-1} - \Delta Q_{\mathrm{SH}}^{-1} = \Delta Q(\boldsymbol{\varkappa}, \boldsymbol{\eta}_{\mathrm{SV}}) - \Delta Q(\boldsymbol{\varkappa}, \boldsymbol{\eta}_{\mathrm{SH}}) \tag{8}$$

TABLE 1
Anisotropy parameters of direct and scattered S-wave absorption for different states of stress *

No.	σ_{xx}	σ_{yy}	σ_{zz}	f								δ
				$Vx90$	$Hx90$	$Vx45$	$Hx45$	$Vy90$	$Hy90$	$Vy45$	$Hy45$	
1	−2	+1	+1	−8	−8	−8	+4	+16	−8	+16	−8	+9
2	−1	−1	+2	+8	−16	+8	−4	+8	−16	+8	−4	+18
3	−1	0	+1	0	−8	0	0	+8	−8	+8	−4	+9
4	−1	+1	0	−8	0	−8	+4	+8	0	+8	−4	0

* Principal axes of tensor σ_{ij} are along coordinate axes x, y (horizontal) and z (vertical). For the state of stress $(-\sigma_{ij})$, e.g. $(2, -1, -1)$ for the first line, signs of f and δ should also be inverted. Indices for f values denote: polarization (V/H), ray azimuth (along x/y) and angle of incidence (45°/90°).

For scattered waves, $D(\boldsymbol{\varkappa})$ can be averaged over $\Omega_{\boldsymbol{\varkappa}}$ with weight $p(\boldsymbol{\varkappa})$ in a similar way as in (6). We denote the result as $\overline{D}$.

Using formulas (7) and (8), a set of calculations were carried out, with the following simplifying assumptions: (1) ρ_0 is isotropic; (2) integration over $\Omega_{\boldsymbol{\varkappa}}$ with weight $p(\boldsymbol{\varkappa})$ can be approximated as averaging by two discrete values of ray azimuth (0° and 90°) and by two values of the angle of incidence (45° and 90°). So, near-vertical ray directions are considered unlikely, and near-horizontal ray directions the most likely.

Calculations were carried out for four variants of static stress (see Table 1), i.e. uniaxial horizontal compression (tension), uniaxial vertical tension (compression) and planar stress with horizontal and vertical intermediate stress axes. Here, we shall assume σ_{ij} as deviator ($\sigma_{ii} = 0$); calculations for hydrostatic load were carried out separately. The accepted stress tensors are given in Table 1 together with the results of the calculations:the values of quantities f and δ that are connected with ΔQ^{-1} and $\overline{D}$ by the relations:

$$\Delta Q^{-1} = \frac{4\pi AB}{105} f, \qquad \overline{D} = \frac{4\pi AB}{105} \delta \tag{9}$$

For hydrostatic load, the result is as one would expect: $f = -7p$, where p is the pressure. In other words, when the pressure increases, cracks close and absorption decreases.

We shall consider now the application of these results to the concentric model of the preparation region. Figure 1 presents a schematic cross section of this region. The precursory dilatancy zone A is assumed to be near to the Earth's surface. The lower boundary of the lithospheric layer which is capable of dilatancy is shown by the wavy line N. The compression zone B with "old" microcracks is also shown, but only the part of it above the N surface should be taken into account. Regions of the medium which are sampled by coda waves are given in two variants, one corresponding to the location of the recording station near to the dilatancy zone A, and the other corresponding to its location at a considerable distance from it. The trajectories of maximum compressive stress are sketched in (dotted lines). It can be seen from the figure that in the first variant it is mainly the dilatancy zone that is sampled, whereas in the second one it is mainly the compressed zone.

The state of crack anisotropy in a dilatancy zone needs careful consideration. In order to obtain the simplest estimate, let us assume that the dilatancy zone is far from the free surface, and that the precursory dilatancy cracks are isotropic. If we take into account the effect of the free surface, we can expect the number of cracks with preferred vertical to increase. This leads to velocity and absorption anisotropy of the same kind as the anisotropy produced by vertical tension of a previously isotropically cracked quasi-Hookean medium. The shear wave absorption anisotropy for such a case is described in line 2 in Table 1, which predicts $\Delta Q_{\mathrm{SV}}^{-1} > \Delta Q_{\mathrm{SH}}^{-1}$.

Suppose that in another case the dilatancy zone is situated initially in the tectonic environment of a horizontal compression (typical for island arcs and the Trans-Eurasian belts). In this case, the intermediate stress axis is directed generally along the structures (horizontally) and the stress state corresponds to line 3 in Table 1. "Steady state"

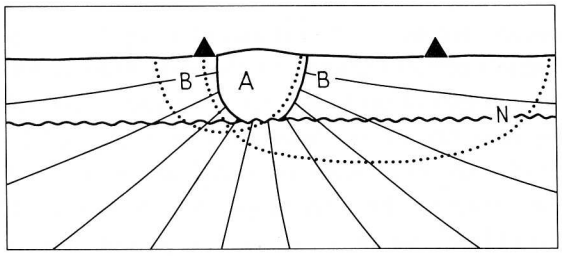

Fig. 1. A schematic cross section of a preparation region. *A*—precursory dilatancy zone; *B*—compression zone; *N*—lower bounding of lithospheric layer capable of dilatancy; solid triangle—station; thin lines—trajectories of maximum compressive stress, dotted lines—rock volumes sampled by coda for two locations of receiver station and sounding shocks near zone A.

cracks are formed here with the same orientation as additional cracks produced (according to (5)) by the same load. Suppose in addition that precursory dilatancy inherits this orientation (crack density is amplified isotropically). Then the anisotropy of the additional absorption of scattered waves (i.e., the sign of the δ value) will also correspond to line 3 in Table 1. Thus, for a compressive tectonic environment, both lines of argument predict the same kind of anisotropy. For shear and the more tensile environments we do not obtain such a definite result.

For the outer compression zone, one can see from Fig. 1 that near the free surface, the state of stress is near to the planar horizontal compression with low σ_{ZZ}. For greater depths, the state of stress becomes closer to unaxial compression along the radii. Hence, the expected effect on scattered waves will lie somewhere between the predictions of lines 1 and 4 in Table 1. Therefore, for a compressive tectonic environment the signs of the expected precursory effects in scattered waves will be the same for both the compression and dilatancy zones, namely $\Delta Q_{SV}^{-1} > \Delta Q_{SH}^{-1}$.

Postulates of initial isotropy and subhorizontal cracks near the free surface in dilatancy zone are, unfortunately, not at all reliable. Experimental data (Crampin et al., 1980, 1984) indicate that in several locations, subvertical dilatancy cracks are the most common. Let us consider this case too. To obtain an estimate, let $\rho_0(\boldsymbol{n})$ in (7) be the "point" delta function on Ω_n, and let only cracks with $\boldsymbol{n} = \{100\}$ be present. Because of azimuthal averaging, the result will be true also for vertical cracks with random orientation. To simulate effects in the dilatancy zone, we can use σ_{ij} corresponding to isotropic tension ($\sigma_{11} = \sigma_{22} = \sigma_{33} = +p$). Making calculations with (7) for a set of χ and averaging, we obtain $\overline{D}$ values again. The set of χ includes two values for between these reflects of incidence as before, but four azimuth values. For the dilatancy zone we obtain $\overline{D} = \Delta Q_{SV}^{-1} - \Delta Q_{SH}^{-1} = -3/8\, AB\rho_0 p$. For the compression zone, the load is again assumed to lie between lines 1 and 4 of Table 1, giving $\overline{D} = 3/32\, AB\rho_0$.

Hence, the calculation for subvertical cracks gives qualitatively different results: first, $\Delta Q_{SV}^{-1} < \Delta Q_{SH}^{-1}$, in the dilatancy zone; and secondly, the sign of the effect in the compression zone is opposite to the sign in the dilatancy zone.

Experimental data supporting the concentric model

Let us now discuss the experimental data (first of all coda wave precursors) from the viewpoint of the above model. We shall associate variations of absorption obtained from coda envelope steepness on any (vertical or horizontal) station channel with Q_S^{-1} values. The difference in the steepness values for between these channels reflects $\overline{D} = \Delta\overline{Q_{SV}^{-1}} - \Delta\overline{Q_{SH}^{-1}}$.

The increase of absorption Q_S^{-1} in the preparation zone of a large earthquake has been estimated by Gusev and Lemzikov (1980; 1984a, b; 1985).

The preparation of three shallow earthquakes with $M \backsim 8$ was studied. In all three cases, the sources and stations were located in the vicinity of the source (and supposedly in the dilatancy zone). We could expect an increase in Q_S^{-1} and some anisotropy, i.e. $\Delta Q_{SV}^{-1} \neq \Delta Q_{SH}^{-1}$. The first effect was very clear ($\Delta Q_S^{-1}/Q_S^{-1} \approx 20\%$ for 1–1.5 years before the main shock), but the second was expressed weakly, and was noted at the nearest station only. The kind of anisotropy was $\Delta Q_{SV}^{-1} > \Delta Q_{SH}^{-1}$, but this result is not very significant.

In Gusev and Lemzikov (1984b) the preparation of a deeper earthquake was studied (Nov. 25, 1971, $M_{LH} = 7.2$, $M_W = 7.8$, near Petropavlovsk, in Kamchatka). Its hypocentral depth was $h = 100$ km, but the probable upper boundary of the finite source was at $h = 40$–50 km. In this case, the coda registered at the nearest station ($\Delta = 40$ km) defi-

nitely shows $\Delta Q_{SV}^{-1} > \Delta Q_{SH}^{-1}$ but at another station (with $\Delta = 100$ km) no clear difference could be seen. A general precursory increase in Q_S^{-1} can also be most clearly seen at the nearest station. Hence, we can suppose that the Kamchatka earthquakes represent the first of the two theoretical cases described in the previous section.

For the same large earthquake, P-wave velocity (V_p) measurements (using explosions) were carried out in the vicinity of its epicentre (Myachkin, 1978). Though no simple pattern of anomalies was observed, one can note that the series of measurements made several months before the main shock (when the coda anomaly was observed) shows a decrease in V_p (compared with the series 1.5 years before and after the event) for the rays nearest to the future source zone, which are most likely to penetrate the dilatancy zone. At the same time, the V_p shows a maximum for the ray farthest from the source (and propagating tangentially). These independent data agree well with the concentric model and enable us to estimate the radius of the dilatancy zone to be 60–100 km in this case, where the source has a length of about 80 km. Coda-wave variations indicating a Q_S^{-1} increase in the preparation region have also been found in other studies (Aki, 1985; Wyss, 1985; Jin and Aki, 1986; Sato, 1986).

Note that Sato (1986) also found a Q_S^{-1} increase for direct waves in the vicinity of a future source (as compared with data obtained at some distance) and that Jin and Aki (1986) were able to determine from their coda shape data not only the Q_S^{-1} increase near the future source but also its decrease around it. This may also explain the observation by Yan and Mo (1984) of increased foreshock duration (normalized to the same M_L) as compared with aftershocks, for an $M = 5.3$ main shock. This result contradicts those of Jin and Aki (1986) and Sato (1986) who used a similar technique. We can infer that a precursory Q_S^{-1} increase does in fact take place, and the concentric model is supported in several cases by observational data.

Another approach to the study of precursory coda wave anomalies was proposed by Malamud (1974) and Mirzoev et al. (1976). They studied time variations in the duration ratio τ_H/τ_Z of near shocks recorded by horizontal and vertical medium-period channels of the same station. Distance ranges of up to $\Delta \doteq 150$ km were considered. Negative precursory anomalies of τ_H/τ_Z of 2–4 months duration were observed in 13 of the 20 cases studied. This technique was also used by Mei (1982) and Ao et al. (1985). In both studies similar precursory anomalies were found. The simplest explanation of the negative anomaly of τ_H/τ_Z is the anisotropic Q_S^{-1} change of the kind $\Delta Q_{SH}^{-1} > \Delta Q_{SV}^{-1}$. This change would be expected for the dilatancy zone in the second theoretical case put forward in the previous section. In general, the problem of precursory Q_S anisotropy needs further study.

In addition to coda wave data, there is much other information to support the concentric model. Gusev et al. (1979) studied the parameter δm_B(equal to $m_b - m_b^*$, where m_b^* is the expected m_b for a given M_S) before four $M = 7.5$–8.0 earthquakes in the Kurile–Kamchatka zone. Positive δm_b may indicate an anomalous high stress drop $\Delta\sigma$. In all four cases, negative δm_b anomalies were found in preparation zones at distances of up to 80–150 km from the future epicentre, with durations of 0.5–1.5 years. The boundary of the anomalous zone was however not found.

Prozorov and Hudson (1983) studied the analogous parameter creepex c (equal to $M_S - M_S^*$, where M_S^* is the expected M_S for a given m_b; $c \approx -2\ \delta m_b$) prior to 21 earthquakes. When the data were averaged with a constant step of 0.5 years, the positive creepex anomaly was found to have a lead time of 1–1.5 years, at distances of up to 110 km from the epicentre, in agreement with the previous paper. No clear pattern was found for greater distances. When, however, a logarithmically changing time step was used in data averaging, a very clear opposite-phased trend of creepex was revealed: an increase within a circle of radius $R < 110$ km and a decrease within the distance range $110 < R < 220$ km from the future epicentre during the period from 1.5 years to 18 days before the main shock.

Analogous results were obtained by Martynov (1983), who discovered a similar opposite-phased trend of $\Delta\sigma$ within and outside an elongated zone of dimensions 6×16 km containing the source of

an impending earthquake of $M = 5$. Khaidarov (1985) also found elongated regions (approx. size 30×100 km) of low-frequency shocks which occurred before two large shocks ($M = 6.6$ and 6.8) in Tienshan. As for the relation of these data to the concentric model, we must admit that so far we have been unable to find any clear theoretical explanation for the δm_b (or $\Delta\sigma$) decrease in the dilatancy zone. A stress drop increase in the compression zone seems to be natural being related to the increase in the stress level as a result of compression.

Wyss and Johnston (1974) found an increase in teleseismic P-wave residuals at two stations situated at 20 and 40 km from the future epicentres of two shocks with $M \approx 6$. In one case, for the rays arriving at the station from two azimuthal sectors, the opposite-phased pattern was found: the average residual anomaly was positive (decreased V_p) for the sector including the epicentre of the future shock; and it was negative (less reliably) for rays tangential to the possible preparation zone. P-wave residuals from local shocks were studied by Motoya (1983) for the preparation zone of an $M = 7$ event. Again the opposite-phased pattern was revealed: V_p increased for rays near to the future source, and decreased for tangential rays. We can also draw attention to the similar result for the Petropavlovsk earthquake cited above.

Mogi (1969) proposed a "doughnut pattern" for precursory seismicity: according to this pattern, activity decreases around the future source zone and increases simultaneously at the periph-

TABLE 2
Estimated size of dilatancy zone and of anomaly duration *

No.	Region and time	n cases	M	$L/2$ (km)	R_d (km)	T_{an}	Kind of precursor	Source
1	Ust–Kamchatsk, Dec. 1971	1	7.8	50	(100)	12 month	coda Q_s	Gusev and Lemzikov, 1980, 1985
2	Kuriles, Oct. 1963; March 1978	2	8	50– 80	(100)	10 and 14 month	coda Q_s	Gusev and Lemzikov, 1984a, 1985
3	Petropavlovsk, Nov. 1971	1	7.2	40	80	1 yr	coda $Q_{SV}^{-1} - Q_{SH}^{-1}$	Gusev and Lemzikov, 1984b
			(7.8)				V_p	Myachkin, 1978
4	Tangshan, Aug. 1976	1	7.8	50	80	3 yr	coda Q_S	Jin and Aki, 1986
5	Yamanashi, Sept. 1983	1	6.3	10	12		Q_S and coda Q_S	Sato, 1986
6	Kalapana, 1975	1	7.2			4 yr	coda Q_S	Wyss, 1985
7	Pamirs, 1969–1973	15	5			2–5 month	τ_H/τ_Z	Malamud, 1974
8	Tangshan, Aug. 1976	1	7.8	50	(85)		τ_H/τ_Z	Mei, 1982
9	Kuriles and Kamchatka, 1971–1973	4	7.5–8	50–100	(100)	0.7–1.5 yr	δm_b	Gusev et al., 1979
10	World, 1971–1978	21	7.5–8	40–150	110	1–1.5 yr	creepex	Prozorov and Hudson, 1983
11	Garm, 1976–1977	2	5	2	3–8 **	3–6 month	$\Delta\sigma$	Martynov, 1983
12	Tienshan, 1970, 1978	2	6.6, 6.8	12	(15–50 **)		$\Delta\bar{\sigma}$	Khaidarov, 1985
13	New Zealand, 1966	2	6	8	20, (40)	1–1.5 yr	P residuals	Wyss and Johnston, 1974
14	Hokkaido, March 1982	1	7.1	25	50	7 yr	P residuals	Motoya, 1983
15	Tangshan, Aug. 1978	1	7.8	50	50–150 **	2–4 yr	el. resistance	Mei, 1982

* R_d is the radius (semi-axis) of the dilatancy zone; values in brackets are determined from the weakening of the effect with distance; R_d values without brackets are based on the opposite-phased effects. T_{an} is anomaly lead time (usually coinciding with its duration).

** Elongated zone, roughly along future earthquake source.

ery of the arising quiescence zone. The doughnut pattern seems to be closely related to the concentric model; if so, the precursory dilatancy suppresses the background seismicity. As in the case of the $\Delta\sigma$ anomaly, we are not able to explain why dilatancy microcracking leads to a decrease in seismicity; however, the increased stress level would explain the increase in seismicity in the outer compression zone.

The coincidence of the quiescence zone and the negative V_p/V_s anomaly zone for several moderate and large earthquakes has been mentioned by Gu (1983). He also proposed that anomalous positive V_p/V_s values often correspond to the edge of the quiescence zone.

For the Tangshan earthquake of 1976, the size of the dilatancy zone can be estimated from four data groups, with a reasonable agreement between four estimates. An anomaly of the τ_H/τ_Z parameter (Mei, 1982) was observed within a circle of $R = 85$ km. A corner in the plot of the B function of Jin and Aki (1986) indicates that the size of the dilatancy zone is of the order of 100 km. This zone can also be located from electrical resistance data (Mei, 1982). The resistance decreases near the future epicentre, but the sign of the anomaly changes at $R = 50$–150 km. In wet conditions, microcracking leads to a decrease in resistance. Hence, the isoline of zero resistance change in Mei (1982) should directly represent the contour of the dilatancy zone. The zone is somewhat elongated and its size is approximately 200×300 km. The doughnut seismicity pattern is observed too; the size of the quiescence zone is 60×100 km (for magnitude level $M = 2$) and the "doughnut" is about 140 km long. The anomaly duration for τ_H/τ_Z is unknown; for each of the other three cases it is about 3 years.

Estimates of the size of the dilatancy zone, anomaly durations and other relevant data are given in Table 2. The value L in this table is the large earthquake source length estimate, either from detailed data or from correlation with M. Generally, after consideration of observational data, the concentric model seems rather reasonable, and one can hope that in some cases it will provide a conceptual basis for the interpretation of the spatial pattern of precursors. Data in Table 2 can also be used to obtain empirical estimates of the ratio of the radius of the dilatancy zone to the half-length of the future source; this ratio seems to range from 1.3 to 3.0, with typical values between 1.5 and 2.0.

Seismic emission—another model for some seismological precursors

There are also coda wave precursors of another kind, which cannot be explained by the model proposed above. Gusev and Lemzikov (1984a, 1985) found "heaps" on average coda envelopes recorded during the coda steepness anomaly before an $M = 7.8$ shock. They interpreted the "heaps" in terms of scattered waves from some very powerful local scatterer until it became clear that the amplitudes were too large to be explained in this way.

In the same two papers it was shown that when the average steepness of coda increases in the preparation period (indicating the probable increase of Q_S^{-1}), the variance of steepness estimates is simultaneously increased. This increase maybe up to four times, and is significant at a level of 5% in one case. This pattern seems to indicate that the coda was a mixture of scattered waves from a small earthquake and of waves from some other origin. The second component influences the estimates of the steepness in a random manner, and gives rise to the "heaps".

In Gusev and Lemzikov (1985), the frequency dependence of coda envelope steepness was studied. The precursory steepness increase is weaker at 1.5 Hz than at 0.75 Hz and almost completely disappears at higher frequencies. This observation contradicts the expected pattern for the case of an increase in intrinsic attenuation, if this attenuation is not frequency selective. Such selectivity seems to be an ad hoc hypothesis. If one relates the steepness increase not to the intrinsic absorption but to increased scattering losses, the phenomenon seems to be explained. However, this explanation is relevant only when the single-scattering approximation is valid. This is not the case here: the multiplicity of scattering is about 2–3 (Gusev and Lemzikov, 1985).

For a diffusion scattering model, which is the relevant one here, the steepness of the coda does

not depend on scattering parameters, and its variations are produced by changes of intrinsic attenuation only. Therefore, we suppose that the described observation is related to some additional radiation source.

We therefore propose that the preparation zone, can produce elastic radiation in some specific way that is different from foreshocks. Noiselike seismic emission was first discussed by Rykunov et al. (1981) for frequencies of 15–30 Hz, and seems to be more likely for lower frequencies.

Seismic emission appears to be present not only in the coda but also in direct waves. Haskell (1966) proposed the introduction of tensile subsources into the model of the earthquake source to explain why P-wave radiation is more powerful than that expected for a shear source—a phenomenon which is most pronounced at high frequencies (Martynov et al., 1979). Against this background of systematic deviations from the shear source model, specific cases only stand out when the deviation becomes abnormally strong, as for example in the case of preparation zones (Nersesov and Semenov, 1969; Potapova and Fedotov, 1974; Fedotov et al., 1977; Ao et al., 1985).

The simplest mechanism for this phenomenon is a tensile motion in the source. Such a model however, does not give a full explanation, as in many cases the relative P-wave amplitudes (even averaged over several stations) are greater than the S-wave amplitudes; and this is impossible even for a pure tensile source. Hence, some other mechanism must be proposed. In our opinion, seismic emission should be employed.

The generation of seismic emission may be related to the formation and disappearance of dilatancy, and the dilatancy zone must be the main source of the seismic emission in the preparation period. The specific modes of emission could be as follows:

Passive emission. A small or large earthquake source formation reduces the shear stress in its vicinity. Since the dilatancy level is determined by the shear stress level, the dilatancy must decrease,

TABLE 3
Expected modes of precursory anomalies *

No.	Precursor	Mode or sign of anomaly	
		dilatancy zone	compression zone
(1) Concentric model			
1	V_p	−	+
2	V_s	anisotropic − on the average	anisotropic + on the average
3	Q_p^{-1}	+	−
4	Q_s^{-1}	anisotropic + on the average	anisotropic − on the average
5	Q_S^{-1} from coda	+	−
6	$Q_{SV}^{-1} - Q_{SH}^{-1}$ from coda	sign is not definite **	
7	Vertical displacement	upwards	complex
8	Horizontal deformation	expansion	compression
9	Pore pressure, level and discharge of wells, ground electric resistance	−	+
10	Stress drop of small shocks, δm_b	−	+
11	Number of small shocks	−	+
(2) Seismic emission model			
12	P/S energy ratio	+	
13	P/S characteristic frequency ratio	+	
14	Stimulated and spontaneous seismic emission	+	

* Dilatancy zone is supposed to be near the surface.

** For $Q_{SV}^{-1} - Q_{SH}^{-1}$, some observations suggest increase and others decrease in the dilatancy zone. The theory can explain any of the results using different initial postulates.

producing passive volume compression and an implosive volume seismic source. Its radiation will mainly consist of P-waves and will add to the radiation of the initial shear source. If a small earthquake occurs in a preparation zone where the dilatancy level is abnormally high, the P/S energy ratio will be abnormally high too.

Active emission. This mechanism represents the stimulation of elastic radiation by an elastic wave. "Active" properties of the medium are related to energy pumping by shear strain. The radiation mechanism itself can be related to the hysteresis of dilatancy, when microcrack formation lags behind the increase of the load. In such cases the elastic wave can initiate the growth of microcracks (up to equilibrium level), and this growth produces the radiation pulse.

Note added in proof

Two new recent reports clearly support the idea of precursory stimulated seismic emission. Both are related to blasts repeatedly fired at the same location and recorded at the same station.

Nikolaev (1986) studied temporal variations of explosion coda in the Tajik region. Two effects similar to the ones described above were revealed: (1) bursts of energy overlap "normal" monotonous coda envelopes during "seismic" periods (formally this phenomenon is demonstrated as an increase in variance of log coda amplitude), and (2) coda Q^{-1} at 0.5–1.5 Hz is greater for "seismic" than for "aseismic" periods, but this difference disappears as frequency increases and the opposite even holds true at 5–7 Hz (the additional HF energy can be seen in the spectra of the coda and of the direct waves).

Magistrale and Kanamori (1986) studied explosion P-waves which propagated through the source region of a $M_L = 5.9$ earthquake. One of the four records contains much more HF energy (of the 3–8 Hz band) than the other three; it was recorded 1 year before the earthquake, and the others, 3 years before and 9 days after it. This picture is not repeated at the other station 25 km away; rays to this station do not penetrate the source region, and all four spectra are alike.

Conclusion

In order to explain several precursory phenomena, two new models of precursor formation are proposed. The first is in essence the logical continuation of the well-known concept of precursory dilatancy; it merely makes the inevitable deduction that the swelling zone of precursory dilatancy must by surrounded by a zone of compression.

The second model is needed to explain some of the coda anomalies which are left aside by the first model. From a seismological point of view, the second model is somewhat radical, since it supposes that the mechanism of seismic radiation, which is different from the usual shear dislocation, is widely spread. The source of radiation of volumetric and the radiation is in P-waves. The new mechanism is thought to be connected with rapid dilatancy variations.

In Table 3, several precursory phenomena are summarized which were either observed and agree with our models, or which could be expected to follow from them.

Acknowledgements

The author is indebted to Professor S.A. Fedotov for encouragement, to V.M. Pavlov, who helped to calculate the f values, to Professors V.N. Nikolaevsky, R.L. Salganik, and to Doctors V.K. Lemzikov, A.G. Prozorov and A.A. Gvozdev for valuable discussions, and to Dr. H. Sato for providing a preprint.

References

Aki, K., 1985. Theory of earthquake prediction with special reference to monitoring of the quality factor of lithosphere by the coda method. Earthquake Predict. Res., 3: 219–230.

Ao Xueming, Wang Guiling and Yang Chenrong, 1985. Anomalous variations of the amplitude ratio characteristics of the seismic wave before and after some strong and moderate earthquakes in Xinjiang, Northwestern Seismol. J., 7 (1): 12–19 (in Chinese).

Artyushkov, E.V., 1982. Geodynamics. Nauka, Moscow (in Russian).

Crampin, S. and Booth, D.C., 1985. Shear wave polarization near the North Anatolian fault. II. Interpretation in terms of crack-induced anisotropy. Geophys. J. R. Astron. Soc., 83: 75–92.

Crampin, S., Evans, R., Ücer, B., Doyle, M., Davis, Y.P., Yegorkina, G.V. and Miller, A., 1980. Observations of dilatancy-induced polarization anomalies and earthquake prediction. Nature, 286: 874–877.

Crampin, S., Evans, R. and Atkinson, B.K., 1984. Earthquake prediction—a new physical basis. Geophys. J. R. Astron. Soc., 76: 147–156.

Fedotov, S.A., Sobolev, G.A., Boldyrev, S.A., Gusev, A.A., Kondratenko, A.M., Potapova, O.V., Slavina, L.B., Theophilaktov, V.D., Khramov, A.A. and Shirokov, V.A., 1977. Long- and short-term earthquake prediction in Kamchatka, Tectonophysics, 37: 305–321.

Gu Jinping, 1983. Seismic velocity anomalies before some strong and moderate earthquakes in province Gansu and its vicinity. Northwest. Seismol. J., 6 (1): 77–83.

Gusev, A.A. and Lemzikov, V.K., 1980. Preliminary results of the study of coda envelope shape of near earthquakes before Ust–Kamchatsk earthquake of 1971. Volcan. Seismol., 1980 (6): 82–93 (in Russian).

Gusev, A.A. and Lemzikov, V.K., 1984a. Anomalies of coda wave characteristics for small earthquakes before three large earthquakes of Kurile–Kamchatka zone, Volcan. Seismol., 1984 (4): 76–90 (in Russian).

Gusev, A.A. and Lemzikov, V.K., 1984b. Coda-wave envelope anomalies of small near earthquakes in preparation zones of Petropavlovsk earthquake of Nov. 24, 1971. Abstr., 4th Conf. Far-East Sect. of MSSS, Yuzhno-Sakhalinsk (in Russian).

Gusev, A.A. and Lemzikov, V.K., 1985. Properties of scattered elastic waves in the lithosphere of Kamchatka: parameters and temporal variations. Tectonophysics, 112: 137–153.

Gusev, A.A., Semenov, A.N. and Sinelnikova, L.G., 1979. The earthquake spectral anomaly estimate by the M_{LH} to m_b relation and its possible application to earthquake prediction. Phys. Earth. Planet. Inter. 18: 326–329.

Haskell, N.A., 1966. Total energy and energy spectral density of elastic wave radiation from propagating faults. 2. A statistical source model. Bull. Seismol. Soc. Am., 56: 125–140.

Jin Anshu and Aki, K., 1986. Temporal change in coda Q before the Tangshan earthquake of 1976, and the Haicheng earthquake of 1975. J. Geophys. Res., 91: 665–675.

Khaidarov, M.S., 1985. Source spectra of Northern Tienshan earthquakes. In: Actual Problems of Geophysics. Nauka, Moscow, pp. 56–66 (in Russian).

Malamud, A.S., 1974. On one possible prognostic feature of large earthquake. Dokl. Akad. Nauk Tajik SSR, 1974 (1) (in Russian).

Magistrale, H. and Kanamori, H., 1986. Changes in NTS seismograms recorded in the source region of the North Palm Springs earthquake of 1986, Eos, Trans. Am. Geophys. Union, 65: 1090.

Martynov, V.G., 1983. S-wave spectra of small local earthquakes, possibility of their use for seismic prediction. In: Experimental Seismology. Nauka, Moscow, pp. 128–142 (in Russian).

Martynov, V.G., Molnar, P., Rautian, T.G. and Khalturin, V.I., 1979. Preliminary results of the study of earthquake spectra of Garm region from the standpoint of the problem of large earthquake prediction. In: Collection of Soviet–American Works on Earthquake Prediction, Vol. 1. Donish, Dushanbe-Moscow, 96–139.

Mei Shirong (Editor), 1982. The Tangshan Earthquake of 1976. Seismol. Press., Beijing, 459 pp.

Mirzoev, K.M., Malamud, A.S., Rura, G.M., Salomov, N.G., Soboleva, O.B. and Starkov, V.I., 1976. Searching for space–time regularities of variations of parameters preceding large earthquakes. In: Earthquake Forerunners Searching. Fan, Tashkent, pp. 241–250 (in Russian).

Mogi, K., 1969. Some features of recent seismic activity in and near Japan (2). Bull. Earthquake Res. Inst., 47: 395–418.

Motoya, Y., 1983. Precursors to the 1982 off Urakawa earthquake, Hokkaido—seismicity, b-value and seismic velocity change. Geophys. Bull. Hokkaido Univ., 42: 263–274.

Myachkin, V.I., 1978. The processes of earthquake preparation. Nauka, Moscow, (in Russian).

Nersesov, I.L. and Semenov, A.N., 1969. Possibility of earthquake prediction by space–time distribution of travel time and amplitude ratio of shear and transverse waves for earthquakes sources of Garm region. Proc. 3rd All-Union Symp. on Seismic Regime, part I. Nauka, Novosibirsk, (in Russian).

Nikolaev, A.V. (Editor), 1986. Seismic Monitoring of the Earth's crust. Institute of Physics of the Earth, Moscow, 290 pp. (in Russian).

Nikolaevsky, V.N., 1982. Earth crust, dilatancy and earthquakes—a review. In: J. Rice, Mechanics of an Earthquake Source. Mir, Moscow (Russian transl.).

Potapova, O.V. and Fedotov, S.A., 1974. Study of the parameter $\theta = \log(E_S/E_P)$ for Kamchatka earthquakes. In: Seismicity, Seismic Prediction, Properties of Upper Mantle and their Relation to Volcanism. Nauka, Novosibirsk, pp. 133–140 (in Russian).

Prozorov, A.G. and Hudson, J.A., 1983. Creepex variations before large earthquakes. Comput. Seismol., 1983 (15). Nauka, Moscow, pp. 26–35 (in Russian).

Rykunov, L.N., Khavrovshkin, O.B. and Tsyplakov, V.V., 1981. Technique and some results of the study of high-frequency microseisms. Volcan. Seismol., 1981 (1): 64–69 (in Russian).

Sato, H., 1986. Temporal change in attenuation intensity before and after the eastern Yamanashi earthquake of 1983 in Central Japan. J. Geophys. Res, 91; 2049–2061.

Scholz, C.H., Sykes, L.R., and Aggarwal, Y.P., 1973. Earthquake prediction: a physical basis. Science, 181: 803–810.

Wyss, M., 1985. Precursory phenomena before large earthquakes. Earthquake Predict. Res., 3: 519–543.

Wyss, M. and Johnston, A.C., 1974. A search for teleseismic P residual changes before large earthquakes in New Zealand. J. Geophys. Res., 79: 3283–3290.

Yan Fendong and Mo Hongjin, 1984. Coda of the 1982 Jianchuan earthquake. J. Seismol. Res., 7 (5): 505–510 (in Chinese).